

Finding Dino: A plug-and-play framework for unsupervised detection of out-of-distribution objects using prototypes

Poulami Sinhamahapatra^{1,2}, Franziska Schwaiger¹, Shirsha Bose^{1,2}, Huiyu Wang¹, Karsten Roscher¹, and Stephan Guennemann²

¹ Fraunhofer IKS, Munich, Germany

² Technical University of Munich, Munich, Germany

Abstract. Detecting and localising unknown or Out-of-distribution (OOD) objects in any scene can be a challenging task in vision. Particularly, in safety-critical cases involving autonomous systems like automated vehicles or trains. Supervised anomaly segmentation or open-world object detection models depend on training on exhaustively annotated datasets for every domain and still struggle in distinguishing between background and OOD objects. In this work, we present a plug-and-play generalised framework - PRototype-based zero-shot OOD detection Without Labels (PROWL). It is an inference-based method that does not require training on the domain dataset and relies on extracting relevant features from self-supervised pre-trained models. PROWL can be easily adapted to detect OOD objects in any operational design domain by specifying a list of known classes from this domain. PROWL, as an unsupervised method, outperforms other supervised methods trained without auxiliary OOD data on the RoadAnomaly and RoadObstacle datasets provided in SegmentMelfYouCan (SMIYC) benchmark. We also demonstrate its suitability for other domains such as rail and maritime scenes.

Keywords: OOD object detection · Anomaly segmentation · Prototype learning

1 Introduction

Artificial Intelligence (AI) has become a cornerstone of autonomous systems - especially in the perception of the surroundings. Systems operating in the real world must dynamically adapt to any situation in open-world settings. This means that in any given scene: the system should be able to understand its context, usually through the detection and localisation of relevant objects. To this end, AI models are typically trained extensively based on object categories in the given operational design domain (ODD). With high-quality publicly available datasets, such as Cityscapes [10], RailSem19 [33] and MODD [4], several State-of-the-Art (SOTA) deep neural networks (DNNs) provide outstanding performances for a closed set of object categories. However, they are unable to identify and categorise unknown objects, i.e. objects that do not belong to any of

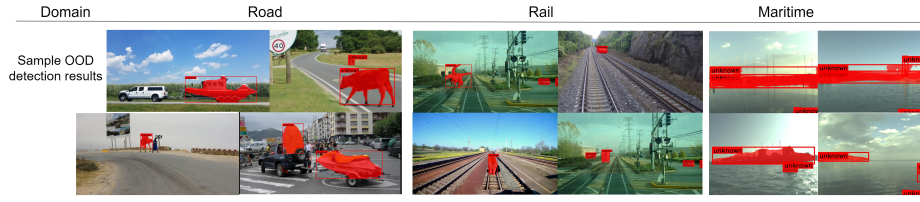


Fig. 1: Sample results for zero-shot unsupervised OOD object detection with PROWL across multiple domains: road driving (test set of RoadAnomaly data from SMIYC benchmark [7]), rail (inpainted OOD on RailSem19 [33]) and maritime scene (marine obstacle detection dataset [4]). All the detected OOD objects are marked as ‘unknown’ in red.

the training classes. One can encounter obstacles that were never learned in the training data like a random animal on the road or unknown floating obstacles in front of unmanned surface vehicles (USVs) in maritime applications. Due to the open world setting, there can be numerous such unknown or out-of-distribution (OOD) objects at any time and it is almost impossible to train DNNs exhaustively with annotated datasets on all possible known object categories and object variations, especially in complex domains such as autonomous driving.

In contrast to image classification, where OOD detection is a well-defined and widely researched topic, the main challenge in the context of camera-based object detection is the explicit distinction between an unknown object and the common *background*, i.e. anything in the scene that is not relevant. Therefore, most existing approaches rely on supervised anomaly segmentation and the use of selected OOD samples during training [1, 8, 22, 28, 30]. Especially the latter is a severe limitation when trying to detect things that were not known at the training time of a model. Open world object detection [14, 17, 34] on the other hand gained some attention recently but is struggling with the application-dependent understanding what a relevant object is.

In this work, we propose a novel framework for the detection of unknown objects in an image: PPrototype-based zero-shot OOD detection Without Labels (PROWL). It can detect an arbitrary number of unknown objects in scenes from any domain in a zero-shot *plug-and-play* manner, i.e. without any additional model training on the target domain, as illustrated in Fig. 1. It leverages the rich and diverse features from pre-trained foundation models such as DINOv2 [27] to robustly capture the known object categories as prototypes in a prototype feature bank. The similarity to those prototypes is then used to calculate a pixel-level similarity score for each given test image. This score can be thresholded to detect OOD pixels. Additionally, we propose to combine foreground masks provided by unsupervised segmentation with those pixel-level scores to refine them into high-quality masks for individual instances of OOD or unknown objects. Making use of pre-trained visual features from foundation models which provide robust representations of almost any object, PROWL can easily generalize across application domains by simply specifying the list of OOD classes to determine the corresponding prototype feature bank. It can unknown

objects without additional model training in just simple inference steps and performs comparably to existing supervised methods. To the best of our knowledge, PROWL is the first end-to-end framework for unsupervised zero-shot OOD detection in any scene without any training in ground truth (GT) classes. Within the framework of PROWL, we compare the performance of several different unsupervised segmentation and detection methods based on the quality of foreground masks generated. In the absence of a direct baseline for unsupervised anomaly segmentation in a multi-object scene, we further compare our results with other supervised segmentation methods from the established SMIYC [7] benchmark based on given metrics and datasets. Further, we show the applicability of PROWL for finding unknowns in diverse scenes like road driving, on railroad tracks, or even maritime.

To summarise, the key contributions of our framework PROWL are:

- PROWL is the first unsupervised OOD object detection and segmentation framework that can sufficiently and reliably distinguish OOD objects from background
- PROWL is a zero-shot OOD object detection framework that relies on pre-trained features from foundation models without additional training on domain data
- PROWL can be applied as an adaptable plug-and-play module generalised to any scene in a new domain without domain-specific training. We demonstrate this by applying to new domains beyond road driving such as rail and maritime domains. For the rail domain, we additionally contribute by creating datasets with inpainted OOD objects
- PROWL outperforms supervised methods trained without auxiliary OOD datasets on the validation sets of RoadAnomaly and RoadObstacle datasets of road driving SMIYC [7] benchmarks as well as shows comparable performance with other supervised methods in Fishyscapes [3] benchmark

2 Related Work

In vision tasks, detecting the unknown/OOD object has been formulated under different banners.

Open World Object Detection (OWOD): As compared to standard closed-world object detection, OWOD poses several challenges such as generating quality candidate proposals on potentially unknown objects or distinguishing the unknown objects from the background. Recent methods [14, 17, 34] have explored probabilistic models based on objectness score of the unknown object and learning novel classes via incremental learning and retraining. But they still have much room for improvement in distinguishing the unknown class from the background.

Anomaly Detection: Anomaly or Out-of-Distribution (OOD) detection was initially conducted in the context of image classification. OOD detection has been widely used for finding deviations from in-distribution (ID), i.e. training data. It encompasses both deviations in distribution shift such as perturbations,

weather, or lighting conditions as well as changes in semantic classes previously not seen during training. Methods originating from image classification focused on developing techniques that aimed to quantify uncertainty in confidence values produced by classification outputs of DNNs (e.g., Maximum Softmax Probability [19], Mahalanobis distance [22]). Other methods find anomalies by estimating the likelihood with generative models [29] or training discriminatively with negative or auxiliary data from OOD samples like ODIN [23], Outlier exposure [20]. Another line of work is finding anomalies or defective parts in an object, such as defective part detection in Industrial Anomaly Detection [25]. Although developed as image-level anomaly / OOD detection, most of these methods can be applied to anomaly segmentation by finding potential anomalies based on the confidences of each pixel.

Anomaly Segmentation: The goal is to predict anomaly probabilities for each pixel in an image. Different works use discriminative or generative approaches [12,24]. Most methods rely on auxiliary out-of-distribution (OOD) data during training. For example, Max Entropy [8] predicts high entropy in anomalous regions and reduces false positives using a meta-classifier on OOD data. DenseHybrid [15] combines discriminative and generative modeling. However, pixel-based reasoning often produces noisy anomaly scores, especially for border pixels and poorly localized anomalies. Recent approaches focus on mask-based methods that capture anomalies as whole objects. These methods predict regions instead of pixels, resulting in fewer false predictions [9]. RbA [26], EAM [16], Maskomaly [1], and Mask2anomaly [28] utilize mask-based classification. However, all these methods are trained with supervised labels and sometimes with OOD data. Our proposed approach eliminates the need to distinguish between ID and OOD object masks. We learn every object as a foreground mask without the notion of OOD/ID object class. We perform unsupervised foreground segmentation and OOD detection separately.

3 Method

In this section, we provide an overview of our framework PROWL. As illustrated in the architecture diagram in Fig. 2, PROWL comprises three modules - a plug-and-play prototype matching module (Sec. 3.2), a refinement module that is used to generate foreground masks using SOTA unsupervised segmentation methods (Sec. 3.1) and lastly OOD detection module (Sec. 3.3).

3.1 Preliminaries: Foreground Mask Generation

In the refinement module, we rely on the generation of foreground masks for every object in the image without considering their respective classes. We find that SOTA unsupervised segmentation methods such as STEGO or CutLER can provide such masks with high quality. Let the foreground masks generated using these methods be denoted as $M = \{m_1, m_2, \dots, m_N\}$. STEGO [18] is an unsupervised semantic segmentation model that distills pre-trained unsupervised visual features from DINO [6] into semantic clusters using contrastive loss, thus discovering and segmenting semantic objects without human supervision for each dataset. CutLER [31] is an approach for training unsupervised object detection

and segmentation models. It is trained exclusively on unlabeled ImageNet [11] data without any additional in-domain data. Using pre-trained self-supervised features, it uses *MaskCut* strategy to discover multiple coarse object masks. Further, it trains a detector through several rounds of self-training to detect multiple foreground objects and corresponding instance segmentation masks. Thus, unlike STEGO, CutLER does not provide dense segmentation as output, rather it provides a zero-shot object detection and instance segmentation for detected foreground objects in the image. Upon varying the detector threshold, CutLER can detect a range of small to large objects.

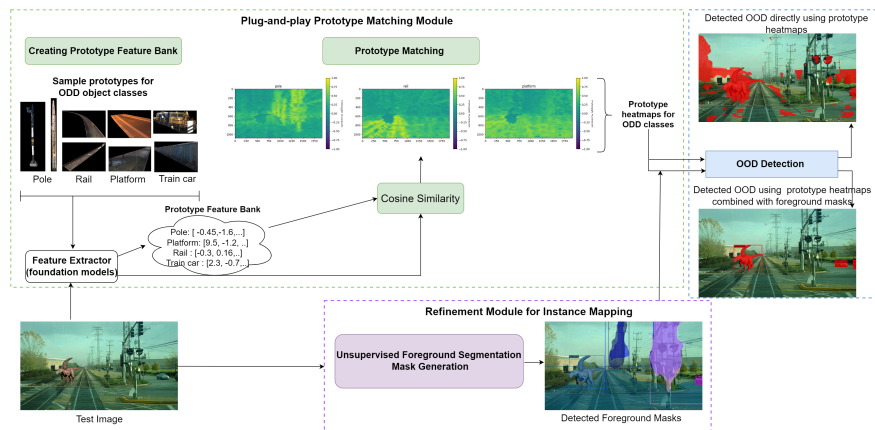


Fig. 2: Overview of our proposed framework PROWL. Firstly, in the plug-and-play prototype matching module, prototype feature bank is created by extracting features from pre-trained foundation models corresponding to few segmented object samples for specified list of OOD object classes. Using this feature bank, prototype matching is performed for the given test image to generate corresponding heatmaps for each object class. Heatmaps show maximum activation (in yellow) wherever the given object is found in test image. In the OOD detection step, the object pixels not satisfying given similarity thresholds are detected as OOD or ‘unknown’ (in red). For less noisy and precise OOD detection, we combine an additional refinement step with prototype heatmaps where foreground masks for every objects in the scene are first extracted in an unsupervised manner. Finally, these foreground masks are detected as either an OOD class or an OOD.

3.2 Plug-and-play Prototype Matching Module

The first step in our pipeline is to create the feature bank with prototypes for every class specified in the OOD. After creation of the prototype, every pixel is assigned a class via prototype matching.

Creating the prototype feature bank: We aim to create an *offline* ‘prototype feature bank’ which are global feature space representation of a specific object class or part of an image. Pre-trained features from foundation models like DINO [6] use knowledge distillation via a teacher-student network for learning in a self-supervised approach. Authors of DINO observe that a self-supervised

Vision Transformer (ViT) can learn to a great extent the underlying perceptual grouping of image patches and semantic correspondences across images and image domains. This property is even strengthened for DINOv2 features [27] which are trained on much larger image corpora and distilled to smaller models. Thus, we utilize the robust general-purpose visual features from DINOv2 for every known object class in ODD using a minimal number of samples from the train split. We assume a list of ODD object categories (expert-specified) that one can expect in a given scene. Let it consist of K known classes $C = \{c_1, c_2, \dots, c_K\}$ and a list of prototype vectors for each class $P = \{p_1, p_2, \dots, p_K\}$. Let us assume L number of samples contribute to each prototype vector p_k for each class c_k . Let the features predicted from a DINOv2 model (g) be $z = g(x)$ for an image x . For each object instance $o_l \in c_k$ class, the segmentation mask s_{o_l} for the instance is extracted, such that each prototype sample image contains only the given object instance with a zeroed-out background, shown in Fig. 2. The features from the region of interest for the object instance are thus calculated as $z_{o_l} = \text{mean}(z * s_{o_l})$. Finally, prototype vector p_k for object class c_k is updated as: $p_k = \{z_{o_l}\}; o_l : l \in \{1, L\}$, i.e. the prototype vector list p_k is extended until L object instances of c_k class is added. This process is repeated for all the K ODD object classes. Depending on the complexity of the dataset, a number of prototype samples can suffice $L \in \{5, 20\}$ for each object (see Sec 5.3) as compared to supervised training methods which require large training samples.

Prototype matching: For each input image x , the inference output z is calculated based on the feature vectors from DINOv2. Now, each pixel is classified into one of the K classes based on cosine similarity between feature vectors of the input image and the prototype vectors P , resulting in K heatmaps one for each class. Thus, the prototype heatmap for class c_k is calculated by taking the maximum of *cosine similarity* between the prototype vectors p_k for respective class and features z given as -

$$h_k = \max(z \cdot p_k) \quad (1)$$

The list of prototype heatmaps for all K ODD classes is given as, $H = \{h_1, h_2, \dots, h_K\}$. For each pixel $[i, j]$ in x , the assigned class label (y) and score (v) is given as:

$$y_{[i,j]} = \text{argmax}(H) \quad (2)$$

$$v_{[i,j]} = \max(H) \quad (3)$$

3.3 OOD Detection

The next step consists of the detection of OOD pixels or object masks following the prototype-based classification of every pixel in Eq 2. This is done by comparing the cosine similarity scores obtained in Eq 3 with a given threshold t , $t \in [0, 1]$. For every pixel we calculate an *inverse normalised cosine similarity* score as:

$$w_{[i,j]} = 1 - \text{norm}(v_{[i,j]}), \text{norm}(x) = \frac{x - \min(x)}{\max(x) - \min(x)} \quad (4)$$

Thus, pixels where $w_{[i,j]} > t$ is designated as an OOD pixel. We have investigated the per-pixel OOD detection performance directly on the prototype heatmaps obtained in according to Equation 1. Although OOD detection based on DINOv2 features can be quite reliable, the resulting OOD detection tends to be noisy, and often the OOD pixels might not precisely localise the relevant object. Thus, the output of PROWL can be further refined by introducing instance-level foreground masks obtained in Sec. 3.1 in combination with the prototype heatmaps. Since these models were trained on huge generic datasets in a self-supervised manner, they can reliably detect multiple foreground object masks in a scene without the notion of known or unknown object class. These masks tend to capture the objectness of every entity in the scene without learning it as background as in supervised detection cases. Thus, every mask m where the majority of pixels is designated as OOD is now considered to be OOD for the entire mask. As shown in Fig. 2, the OOD objects *dinosaur* and *passenger car* were correctly detected using prototype heatmaps in PROWL as they did not match with any of the classes listed in the prototype bank, however, additional pixels were also spuriously detected as OOD. While PROWL in combination with foreground masks from CutLER, correctly detected and precisely localised the exact OOD object masks as ‘unknown’.

4 Implementation Details

4.1 Datasets

We demonstrate the plug-and-play performance of our methods by evaluating them in three different operational design domains (ODD).

Road driving scene - We generated prototypes for the urban driving road ODD scene from **Cityscapes** [10]. It is a benchmark suite with both pixel and instance-level semantic scene understanding. For evaluation on datasets with real OOD objects in the road scene, we refer to the datasets and benchmark suite for anomaly segmentation in *SegmentMeIfYouCan* (SMIYC) [7]. It provides two novel real-world datasets: **RoadAnomaly21** and **RoadObstacle21**. RoadAnomaly21 consists of 100 test and 10 validation images with real objects or animals as OOD appearing anywhere in the scene. In contrast, RoadObstacle21 has OOD objects (or obstacles) appearing on the road or ego track. The authors of SMIYC withhold the GT for the test set, where the scores are only accessible by submitting the method to the official benchmark. Further, we also evaluate on **FS Static** subset of **Fishyscapes** [2] anomaly segmentation benchmark. It consists of 30 validation images with generic objects taken from PASCAL VOC [13] synthetically overlaid on Cityscapes images.

Rail scene - For rail ODD, we use **RailSem19** [33] dataset which provides diverse images taken from an ego-perspective of a rail vehicle (trains or trams) along with extensive semantic annotations including rails. Regarding OOD detection, there exist no publicly available datasets with OOD objects in the rail scene yet. Thus, we create our validation data consisting of 10 images. We have used Inpaint Anything [32] which uses a combination of SAM, LaMa, and Stable Diffusion, for inpainting potential OOD objects like animals, cars, carts etc on to the RailSem19 images. More details are given in Suppl.

Maritime scene - Obstacle detection and segmentation in maritime ODD (MODD) scenario is prevalent for autonomous operations of unmanned surface vehicles (USVs). Here, the task is to detect and segment all obstacles beyond *sky*, *sea* classes as ‘unknown’. We formulate this as an OOD detection task, where prototypes are generated from train split of **MaStr1325** (Maritime Semantic Segmentation Training Dataset) [4]. For OOD detection evaluation, we evaluate on corresponding test dataset. We do not compare with MODS benchmark [5] as we do not include evaluations taking into account multi-modal data with IMU calibrations for shoreline detection.

4.2 Experimental Setup

PROWL is a zero-shot method, which means it does not rely on any training but merely some inference steps. The ViT-S/14 of DINO-v2 [27] pre-trained on a dataset of 142 million images is taken as the feature extractor of PROWL. We observe that with a default inverse cosine similarity threshold (Eq. 4) at 0.55 and CutLER detector threshold of 0.2, we obtain a general satisfactory performance across all the datasets. We further report that depending upon the size of the OOD objects and complexity of the OOD datasets, this optimal threshold tends to suffice even at higher values as shown in the ablation study for OOD datasets for Cityscapes (Sec 5.3).

4.3 Evaluation metric

To the best of our knowledge, there exists no prior work on unsupervised OOD detection from multiple objects in a scene. Thus, there are no established benchmarks and evaluation metrics for the task. The Area under the Receiver Operating Characteristic (AUROC) curve is a standard metric for OOD detection for image classification. However, in the case of multiple OOD object detection and segmentation tasks with a highly imbalanced number of OOD objects, the Area under the Precision-Recall Curve (AUPRC) is a more suitable choice. Thus, to compare with Anomaly Segmentation metrics provided with the SMIYC benchmark, we use AUPRC and False Positive Rate at True Positive Rate of 95% (FPR) metrics for pixel-wise evaluation. Further, for evaluation as a binary segmentation task, we select a fixed inverse cosine similarity threshold for all the datasets and predict 1 (positive) for pixels determined as OOD otherwise 0. This binary prediction mask is compared with the GT mask and evaluated using mean Intersection over Union (mIoU) and F1 score.

5 Results and Discussion

In this section, we show different experiments to evaluate the performance of PROWL for OOD detection. In Sec. 5.1, we present results comparing with State-of-the-Art (SOTA) supervised methods in the road driving scene reported in the existing anomaly segmentation benchmarks SMIYC [7]. In Sec. 5.2, we show the applicability of PROWL into other domains such as rail and maritime scenes where there are no directly comparable benchmarks. Lastly, in Sec 5.3, we provide ablation for different hyper-parameters and strategies used in our implementation.

We report results for our method PROWL in two scenarios as explained in Sec. 3.3: (a) PROWL (Without foreground masks) - OOD pixels are directly obtained by thresholding the scores from prototype heatmaps, (b) PROWL + refinement module using foreground masks - The foreground masks generated by unsupervised segmentation methods (STEGO [18], CutLER [31] as applicable) are combined with prototype heatmaps, such that individual masks (not pixels) are detected as OOD objects or not.

5.1 Comparison with the State-of-the-Art on road driving scene

In the road driving scene, we evaluate on datasets with real OOD objects like RoadAnomaly21 and RoadObstacle21 provided by SMIYC benchmark [7] and the synthetic OOD objects in FS-Static given in Fishyscapes [3] benchmark. We created prototype bank for road scene using 19 OOD classes from Cityscapes, in accordance with the classes recommended in SMIYC following [10].

Method	Seg. type	Aux. data	RoadAnomaly		FS Static		RoadObstacle	
			AUPR	FPR	AUPR	FPR	AUPR	FPR
<i>Supervised</i>								
PEBAL	Pixel	✓	45.1	44.6	92.1	1.5	-	-
Max. Entropy	Pixel	✓	79.7	19.3	76.3	7.1	-	-
DenseHybrid	Pixel	✓	63.9	43.2	60.0	4.9	-	-
M2A	Mask	✓	79.7	13.5	-	-	-	-
EAM	Mask	✗	66.7	13.4	<u>87.3</u>	<u>2.1</u>	-	-
Maskomaly	Mask	✗	<u>70.9</u>	<u>11.9</u>	69.5	14.4	0.96*	92.10*
<i>Unsupervised</i>								
PROWL	Pixel	✗	45.98	26.58	<u>61.08</u>	<u>20.28</u>	11.10	46.97
PROWL + STEGO	Mask	✗	<u>53.97</u>	<u>13.52</u>	45.6	26.25	40.15	14.11
PROWL + CutLER	Mask	✗	75.25	1.75	73.29	1.46	75.43	1.84

Table 1: Results on RoadAnomaly, FS Static and RoadObstacles on the validation set. We separate the methods based on supervision needed during training. The best results are marked in bold, and second best are underlined for each category. * indicates reproduced results with official code and checkpoints. PROWL+ CutLER outperforms unsupervised variants in all datasets as well as supervised methods trained without auxiliary data on RoadAnomaly and RoadObstacle.

To the best of our knowledge, there are no other *unsupervised* OOD object detection methods comparable as a baseline to our method. Thus, it should be noted that all the methods used for comparison with SOTA are supervised, i.e. these models are trained on semantic annotations of the 19 classes of Cityscapes, whereas we rely on few inference steps based on prototype features from DINOv2.

In Table 1, we compare results reported by other supervised methods on the validation set of respective OOD datasets. The metrics used are threshold-independent metrics such as AUPR and FPR at the best TPR (or 95%). We note that while the other reported metrics are based on probabilistic confidence scores, we calculate positives (OOD pixels) by varying the inverse cosine similarity threshold in Eq. 4. Thus, we are unable to compare with the test set of the benchmark due to non-compatibility with expected probabilistic inputs on the official benchmark code. We indicate the segmentation type of each method as pixel or mask-based. Further, many SOTA methods achieve superior results by discriminatively training with *auxiliary data*, i.e., exposed to few OOD samples

as negative data. We include those SOTA methods with backbones having similar predictive power in evaluation and are ranked higher in the SMIYC benchmark. For comparison purposes, we assume *Maskomaly* [1] as our direct *supervised baseline* as it is also a zero-shot inference based approach like PROWL, depending on pre-trained Mask2Former [9] model on Cityscapes. Unlike other methods, it provided SOTA results on RoadAnomaly amongst the methods not trained with auxiliary data.

We show that PROWL with CutLER performs best compared to all the other variants amongst the unsupervised methods. In comparison to *supervised methods trained without auxiliary data*, PROWL outperforms on the RoadAnomaly and RoadObstacle datasets. It provides overall best FPR for RoadAnomaly across all methods and +4.35% *gain in AUPR*. For FS Static, our unsupervised methods perform quite comparable to supervised methods (second best) and performs better than Maskomaly as well. We note that most supervised methods do not report results on validation set for RoadObstacles and the reproduced results for Maskomaly show poor performance, also shown in Fig 3.

Method	Supervised	RoadAnomaly		FS Static		RoadObstacle	
		mIoU	F1	mIoU	F1	mIoU	F1
Maskomaly*	Yes	46.86	56.76	23.97	29.92	9.31	11.29
PROWL	No	38.46	54.68	39.43	50.75	6.79	11.21
PROWL + STEGO	No	56.24	69.81	39.21	49.9	29.92	35.10
PROWL + CutLER	No	75.22	85.25	64.79	72.18	49.16	53.31

Table 2: Performance of our unsupervised methods compared to supervised baseline for binary segmentation with fixed thresholds on the validation set of OOD datasets. * indicates reproduced results with official code and checkpoints with a threshold of 0.9. PROWL + CutLER outperforms across all datasets.

In Table 2 and Fig. 3, we present the comparative performance of our methods against supervised SOTA baseline (Maskomaly [1]) as a binary segmentation task. For this, we compare the binary GT masks with OOD pixels given as 1 with the binary masks generated from the pixels predicted as OOD by different methods. We evaluate mIoU and F1 scores with fixed inverse cosine similarity thresholds on the best threshold for validation set of respective OOD datasets for Cityscapes (Fig. 5c). The authors of Maskomaly [1] report results on the validation set by calculating best threshold per-image by checking best F1 score using GT. However, for fair comparison we reproduce all the results for Maskomaly with their reported fixed confidence threshold of 0.9.

In Table 2, we show that PROWL with CutLER outperforms other unsupervised variants as well as supervised baseline in terms of both mIoU and F1 scores with a significant margin. We observe that there’s an overall decreasing trend of performance in most methods across OOD datasets from RoadAnomaly, FS-Static to RoadObstacle. This can be attributed also to the difficulty of the dataset and the size of OOD object within the image. We can correlate this with the qualitative results provided in Fig. 3. RoadAnomaly dataset provides real OOD objects which are comparably big like the *carriage* or *helicopter* but also in a scene different than the city roads in Cityscapes. Thus, while bigger OOD

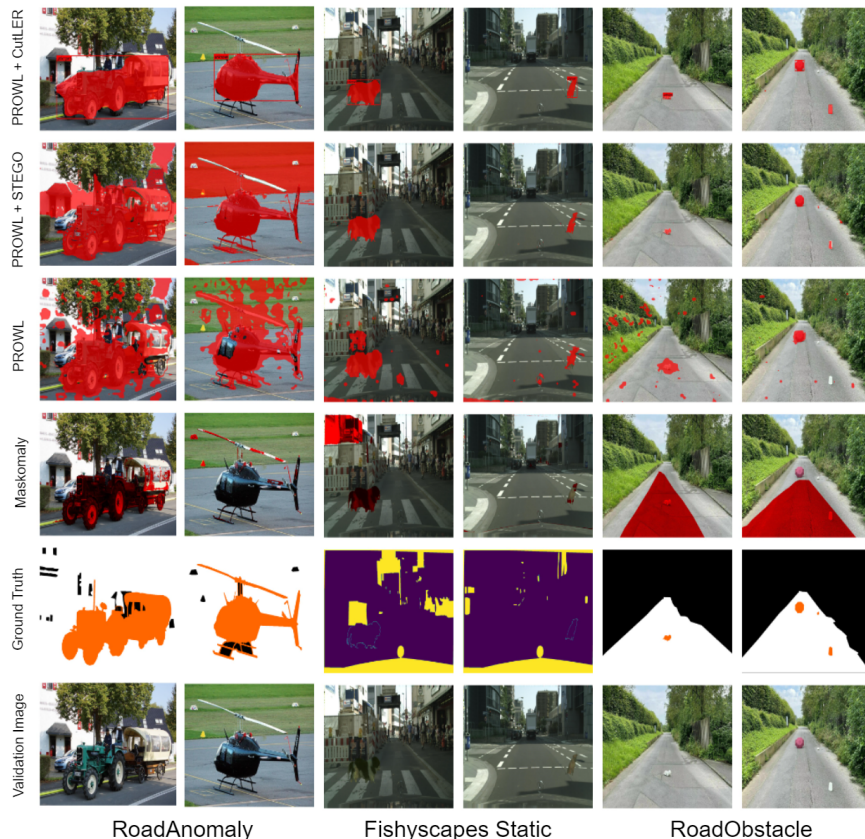


Fig. 3: Qualitative comparison of different unsupervised methods with PROWL as compared to supervised baseline Maskomaly. Results generated using fixed thresholds on the validation set of RoadAnomaly, FS Static and RoadObstacles datasets. Detected OOD pixel segmentations shown in red. PROWL+CutLER provides qualitatively superior OOD detection and segmentation across all datasets.

objects are easier to detect, the background objects might also be often detected as OOD. We observe this trend for results corresponding to prototype heatmaps in PROWL and STEGO with PROWL. Although Maskomaly reports good results on SMIYC benchmark, we still observe that the masks detected for OOD are highly insufficient with only partial detections. In contrast, since CutLER detects foreground object boxes and then provides semantic masks, the entire mask is precisely detected as OOD object using PROWL. For FS-Static, the OOD objects are synthetic images which often have a matching texture with the background of Cityscapes test images. So, although most methods do not falsely predict too many background pixels as OOD, we see some false predictions in the background for Maskomaly and PROWL in the image of *dog crossing the road*. The primary difficulty in this dataset could be missing the OOD object due to similar texture as background. This is apparent for the Maskomaly image with *dog sitting on road*. Overall, STEGO with PROWL performs quite nicely,

as STEGO has learnt via contrastive clustering to find semantic correspondences in foreground masks on Cityscapes and thus nicely finds small semantic masks which are significantly different rather than bigger deviations in the scene as in RoadAnomaly. We observe that CutLER with PROWL precisely detects the OOD masks in most cases. For the RoadObstacle dataset, the OOD objects are meant as real obstacles of small sizes and varying numbers placed on the ego-track at different distances. Due to smaller sizes with increasing distance, all methods show worse performance as compared to other datasets. The reproduced Maskomaly results falsely captures most of the road. PROWL finds the OOD objects in most cases but also falsely predicts many background pixels as OOD. We observe the superior qualitative performance of object masks provided by STEGO and CutLER which helps in localising the objects as entire masks and then detecting them as OOD via PROWL. We note although STEGO localises all the OOD object masks, the semantic masks are somewhat discontinuous. In comparison, CutLER with PROWL precisely localises and segments the OOD object masks, justifying the overall better performance. Although vanilla PROWL is quite close to detecting the OOD pixels, however with above examples we show that the additional unsupervised foreground masks helping in refining the OOD object masks avoiding spurious false predictions.

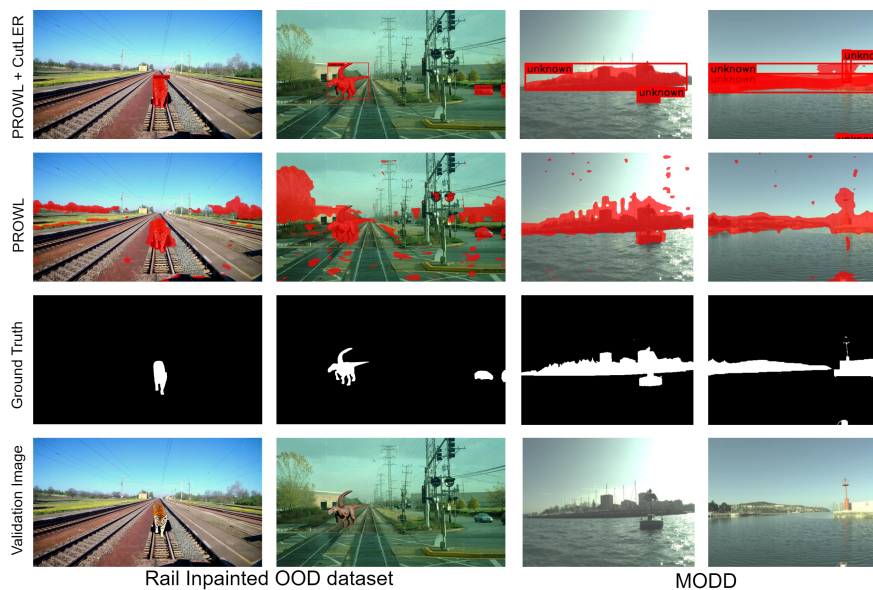


Fig. 4: Qualitative results for zero-shot OOD detection in other OOD domains - rail and maritime scene. Detected OOD pixel segmentations are depicted in red colour.

5.2 Evaluation of plug and play application to other domains

To demonstrate zero-shot plug-and-play application of PROWL to other domains, we extend our evaluation to rail and maritime OOD scene with respective OOD datasets given in Sec. 4.1. For rail OOD, we use the dataset created with inpainted OOD objects. For simplicity, we consider the following 6 predominant

classes in RailSem19 [33] for creating prototype bank of known classes - *train car, platform, rail, fence, person, pole*. Similarly, for maritime we refer to MODD [4] and create prototype bank with *sky, sea* as known OOD classes. Every other object is OOD. Since there exists no benchmark on RailSem19 OOD detection and the MODS [5] uses separate evaluation strategy, we provide evaluation using our zero-shot methods with PROWL. Since CutLER models were trained without labels only on ImageNet [11], it can easily provide zero-shot inference on any domain, whereas STEGO still needs to train on the datasets of new domain although without labels. Similarly, our supervised baseline Maskomaly [1] relies on Mask2Former which still needs to train with the labels of the respective training data, thus can not be readily used for comparison.

Method	Supervised	Rail Inpainted OOD		MODD	
		mIoU	F1	mIoU	F1
PROWL	No	8.01	14.33	62.35	76.36
PROWL + CutLER	No	83.29	90.38	73.30	84.08

Table 3: Performance of our unsupervised methods in other domains such as rail and maritime scenes for binary segmentation with fixed thresholds on the validation datasets. * indicates reproduced results with official code and checkpoints with a threshold of 0.9.

In Table 3, we show the performance of PROWL vs CutLER with PROWL as a binary segmentation task using fixed similarity threshold for detection of OOD pixels. We find that CutLER with PROWL performs better as compared to vanilla PROWL in both cases. In Fig. 4, we show corresponding qualitative results. We observe that PROWL is significantly worse in case Rail Inpainted OOD data as compared to MODD where it performs quite comparably as CutLER with PROWL. This could be attributed to the fact that prototype heatmaps in PROWL provide per-pixel outputs, causing false positives to the background objects like *vegetation, buildings* that are not in the assumed OOD class list. CutLER provides an advantage here, where the relevant object masks (including OOD) can be filtered based on foreground score while irrelevant background objects can be ignored. However, in MODD dataset, the task is relatively simple as everything other than *sea, sky* should be detected as OOD or obstacle, thus both methods perform well on this dataset.

5.3 Ablations

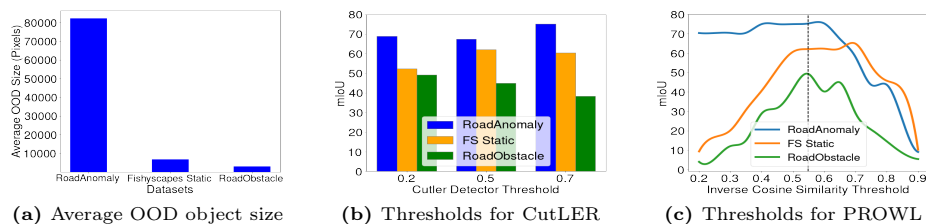


Fig. 5: Ablation Study: a) Variation of OOD size, b) Performance of PROWL with variation of Cutler Detector Threshold, c) Performance of PROWL with variation of Inverse Similarity Threshold, across all OOD datasets for Cityscapes.

In Fig.5, we show ablation study for different hyperparameters used in the experiments with PROWL depending upon complexity of different OOD datasets, such as variation of average OOD object size in pixels Fig. 5a where RoadAnomaly shows much bigger objects as compared to RoadObstacle with smaller objects. Fig.5b shows CutLER thresholds for generating optimal number of foreground masks for PROWL with the inverse cosine similarity threshold set at 0.55. Optimal mIoU is achieved for CutLER thresholds of 0.7, 0.5, and 0.2 for RoadAnomaly, FS Static, and RoadObstacle datasets respectively. This trend is justifiable as smaller objects require lesser thresholds so as to detect maximum object masks, whereas bigger objects can be reliably detected even with higher detector thresholds. In Fig. 5c, we fix the CutLER thresholds given above and find the optimum inverse cosine similarity threshold for best OOD detection based on mIoU. We observe FS Static peaks at relatively high threshold of 0.7 as the dataset is quite similar to ID Cityscapes data, whereas RoadAnomaly and RoadObstacle dataset peak at 0.55, 0.60 respectively close to the default threshold at 0.55.

Lastly Fig. 6, shows the performance of PROWL with varying number of prototype samples used to create the prototype feature bank for the Cityscapes dataset in road driving domain. We show already quite good AUPRC is achieved with as less as 5 prototypes and it starts to saturate from 15 and above. For our experiments, 20 samples per ODD class were used for Cityscapes. For RailSem19 and MODD datasets with less complexity and lesser number of ODD classes, approximately 10 prototype samples were found to be sufficient.

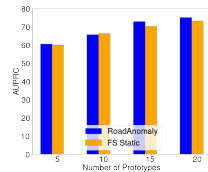


Fig. 6: Performance of PROWL with variation in the number of prototype samples

6 Conclusion

In this work, we proposed the first unsupervised OOD object detection and segmentation framework - PROWL. It is a zero-shot plug-and-play framework which can be easily transferred to different domains without further training on domain specific data. Since it relies on extracting prototype features from foundation models, it stands as a practical approach towards many open world settings. We show that PROWL combined with CutLER outperforms all the unsupervised as well supervised methods (trained without auxiliary OOD data) on the SMIYC validation set in road driving scenes. With different OOD datasets, we show that it can detect real OOD objects of different sizes (RoadObstacle) as well as diverse scenes (RoadAnomaly). By applying it to rail and maritime applications, we demonstrate that it can be easily adapted to other domains. Even with a limited number of classes and prototypes defined in our OOD setting, PROWL performs reliably on the available benchmarks. However, due to the limited availability of diverse and high quality data sets for evaluation, a next step would be to put PROWL to the test in diverse scenarios with extensively defined OOD. Further, we clearly identified a need for harmonized evaluation metrics and settings to enable a fair comparison of approaches in the future.

References

1. Ackermann, J., Sakaridis, C., Yu, F.: Maskomaly:Zero-Shot Mask Anomaly Segmentation (Aug 2023). <https://doi.org/10.48550/arXiv.2305.16972>
2. Blum, H., Sarlin, P.E., Nieto, J., Siegwart, R., Cadena, C.: Fishyscapes: A Benchmark for Safe Semantic Segmentation in Autonomous Driving. In: 2019 IEEE/CVF International Conference on Computer Vision Workshop (ICCVW). pp. 2403–2412. IEEE, Seoul, Korea (South) (Oct 2019). <https://doi.org/10.1109/ICCVW.2019.00294>
3. Blum, H., Sarlin, P.E., Nieto, J., Siegwart, R., Cadena, C.: The Fishyscapes Benchmark: Measuring Blind Spots in Semantic Segmentation. *Int J Comput Vis* **129**(11), 3119–3135 (Nov 2021). <https://doi.org/10.1007/s11263-021-01511-6>
4. Bovcon, B., Muhovic, J., Pers, J., Kristan, M.: The MaSTr1325 dataset for training deep USV obstacle detection models. In: 2019 IEEE/RSJ International Conference on Intelligent Robots and Systems (IROS). pp. 3431–3438. IEEE, Macau, China (Nov 2019). <https://doi.org/10.1109/IROS40897.2019.8967909>
5. Bovcon, B., Muhovič, J., Vranac, D., Mozetič, D., Perš, J., Kristan, M.: MODS – A USV-oriented object detection and obstacle segmentation benchmark. *IEEE Trans. Intell. Transport. Syst.* **23**(8), 13403–13418 (Aug 2022). <https://doi.org/10.1109/TITS.2021.3124192>
6. Caron, M., Touvron, H., Misra, I., Jegou, H., Mairal, J., Bojanowski, P., Joulin, A.: Emerging Properties in Self-Supervised Vision Transformers. In: 2021 IEEE/CVF International Conference on Computer Vision (ICCV). pp. 9630–9640. IEEE, Montreal, QC, Canada (Oct 2021). <https://doi.org/10.1109/ICCV48922.2021.00951>
7. Chan, R., Lis, K., Uhlemeyer, S., Blum, H., Honari, S., Siegwart, R., Fua, P., Salzmann, M., Rottmann, M.: SegmentMeIfYouCan: A Benchmark for Anomaly Segmentation
8. Chan, R., Rottmann, M., Gottschalk, H.: Entropy Maximization and Meta Classification for Out-of-Distribution Detection in Semantic Segmentation. In: 2021 IEEE/CVF International Conference on Computer Vision (ICCV). pp. 5108–5117. IEEE, Montreal, QC, Canada (Oct 2021). <https://doi.org/10.1109/ICCV48922.2021.00508>
9. Cheng, B., Misra, I., Schwing, A.G., Kirillov, A., Girdhar, R.: Masked-attention Mask Transformer for Universal Image Segmentation. In: 2022 IEEE/CVF Conference on Computer Vision and Pattern Recognition (CVPR). pp. 1280–1289. IEEE, New Orleans, LA, USA (Jun 2022). <https://doi.org/10.1109/CVPR52688.2022.00135>
10. Cordts, M., Omran, M., Ramos, S., Rehfeld, T., Enzweiler, M., Benenson, R., Franke, U., Roth, S., Schiele, B.: The Cityscapes Dataset for Semantic Urban Scene Understanding. In: 2016 IEEE Conference on Computer Vision and Pattern Recognition (CVPR). pp. 3213–3223. IEEE, Las Vegas, NV, USA (Jun 2016). <https://doi.org/10.1109/CVPR.2016.350>
11. Deng, J., Dong, W., Socher, R., Li, L.J., Li, K., Fei-Fei, L.: ImageNet: A large-scale hierarchical image database. In: 2009 IEEE Conference on Computer Vision and Pattern Recognition. pp. 248–255 (Jun 2009). <https://doi.org/10.1109/CVPR.2009.5206848>
12. Di Biase, G., Blum, H., Siegwart, R., Cadena, C.: Pixel-wise Anomaly Detection in Complex Driving Scenes. In: 2021 IEEE/CVF Conference on Computer Vision and Pattern Recognition (CVPR). pp. 16913–16922. IEEE, Nashville, TN, USA (Jun 2021). <https://doi.org/10.1109/CVPR46437.2021.01664>

13. Everingham, M., Van Gool, L., Williams, C.K.I., Winn, J., Zisserman, A.: The Pascal Visual Object Classes (VOC) Challenge. *Int J Comput Vis* **88**(2), 303–338 (Jun 2010). <https://doi.org/10.1007/s11263-009-0275-4>
14. Fontanel, D., Tarantino, M., Cermelli, F., Caputo, B.: Detecting the unknown in Object Detection (Aug 2022)
15. Grcić, M., Bevandić, P., Šegvić, S.: DenseHybrid: Hybrid Anomaly Detection for Dense Open-set Recognition (Jul 2022)
16. Grcić, M., Šarić, J., Šegvić, S.: On Advantages of Mask-level Recognition for Outlier-aware Segmentation. In: 2023 IEEE/CVF Conference on Computer Vision and Pattern Recognition Workshops (CVPRW). pp. 2937–2947. IEEE, Vancouver, BC, Canada (Jun 2023). <https://doi.org/10.1109/CVPRW59228.2023.00295>
17. Gupta, A., Narayan, S., Joseph, K.J., Khan, S., Khan, F.S., Shah, M.: OW-DETR: Open-world Detection Transformer. In: 2022 IEEE/CVF Conference on Computer Vision and Pattern Recognition (CVPR). pp. 9225–9234. IEEE, New Orleans, LA, USA (Jun 2022). <https://doi.org/10.1109/CVPR52688.2022.00902>
18. Hamilton, M., Zhang, Z., Hariharan, B., Snavely, N., Freeman, W.T.: UNSUPERVISED SEMANTIC SEGMENTATION BY DISTILLING FEATURE CORRELATIONS (2022)
19. Hendrycks, D., Gimpel, K.: A Baseline for Detecting Misclassified and Out-of-Distribution Examples in Neural Networks (Oct 2018). <https://doi.org/10.48550/arXiv.1610.02136>
20. Hendrycks, D., Mazeika, M., Dietterich, T.: Deep Anomaly Detection with Outlier Exposure (Jan 2019). <https://doi.org/10.48550/arXiv.1812.04606>
21. Kirillov, A., Mintun, E., Ravi, N., Mao, H., Rolland, C., Gustafson, L., Xiao, T., Whitehead, S., Berg, A.C., Lo, W.Y., Dollár, P., Girshick, R.: Segment Anything. In: 2023 IEEE/CVF International Conference on Computer Vision (ICCV). pp. 3992–4003. IEEE, Paris, France (Oct 2023). <https://doi.org/10.1109/ICCV51070.2023.00371>
22. Lee, K., Lee, K., Lee, H., Shin, J.: A Simple Unified Framework for Detecting Out-of-Distribution Samples and Adversarial Attacks (Oct 2018). <https://doi.org/10.48550/arXiv.1807.03888>
23. Liang, S., Li, Y., Srikant, R.: Enhancing The Reliability of Out-of-distribution Image Detection in Neural Networks (Aug 2020). <https://doi.org/10.48550/arXiv.1706.02690>
24. Lis, K., Nakka, K.K., Fua, P., Salzmann, M.: Detecting the Unexpected via Image Resynthesis. In: 2019 IEEE/CVF International Conference on Computer Vision (ICCV). pp. 2152–2161. IEEE, Seoul, Korea (South) (Oct 2019). <https://doi.org/10.1109/ICCV.2019.00224>
25. Liu, J., Xie, G., Wang, J., Li, S., Wang, C., Zheng, F., Jin, Y.: Deep Industrial Image Anomaly Detection: A Survey. *Mach. Intell. Res.* **21**(1), 104–135 (Feb 2024). <https://doi.org/10.1007/s11633-023-1459-z>
26. Nayal, N., Yavuz, M., Henriques, J.F., Güney, F.: RbA: Segmenting Unknown Regions Rejected by All. In: 2023 IEEE/CVF International Conference on Computer Vision (ICCV). pp. 711–722. IEEE, Paris, France (Oct 2023). <https://doi.org/10.1109/ICCV51070.2023.00072>
27. Oquab, M., Darcet, T., Moutakanni, T., Vo, H.V., Szafraniec, M., Khalidov, V., Fernandez, P., Haziza, D., Massa, F., El-Nouby, A., Assran, M., Ballas, N., Galuba, W., Howes, R., Huang, P.Y., Li, S.W., Misra, I., Rabbat, M., Sharma, V., Synnaeve, G., Xu, H., Jegou, H., Mairal, J., Labatut, P., Joulin, A., Bojanowski, P.: DINOv2: Learning Robust Visual Features without Supervision

28. Rai, S.N., Cermelli, F., Fontanel, D., Masone, C., Caputo, B.: Unmasking Anomalies in Road-Scene Segmentation
29. Ren, J., Liu, P.J., Fertig, E., Snoek, J., Poplin, R., Depristo, M., Dillon, J., Lakshminarayanan, B.: Likelihood Ratios for Out-of-Distribution Detection. In: Advances in Neural Information Processing Systems. vol. 32. Curran Associates, Inc. (2019)
30. Tian, Y., Liu, Y., Pang, G., Liu, F., Chen, Y., Carneiro, G.: Pixel-wise Energy-biased Abstention Learning for Anomaly Segmentation on Complex Urban Driving Scenes (Sep 2022). <https://doi.org/10.48550/arXiv.2111.12264>
31. Wang, X., Girdhar, R., Yu, S.X., Misra, I.: Cut and Learn for Unsupervised Object Detection and Instance Segmentation. In: 2023 IEEE/CVF Conference on Computer Vision and Pattern Recognition (CVPR). pp. 3124–3134. IEEE, Vancouver, BC, Canada (Jun 2023). <https://doi.org/10.1109/CVPR52729.2023.00305>
32. Yu, T., Feng, R., Feng, R., Liu, J., Jin, X., Zeng, W., Chen, Z.: Inpaint Anything: Segment Anything Meets Image Inpainting (Apr 2023). <https://doi.org/10.48550/arXiv.2304.06790>
33. Zendel, O., Murschitz, M., Zeilinger, M., Steininger, D., Abbasi, S., Beleznai, C.: RailSem19: A Dataset for Semantic Rail Scene Understanding. In: Proceedings of the IEEE/CVF Conference on Computer Vision and Pattern Recognition Workshops. pp. 0–0 (2019)
34. Zohar, O., Wang, K.C., Yeung, S.: PROB: Probabilistic Objectness for Open World Object Detection. In: Proceedings of the IEEE/CVF Conference on Computer Vision and Pattern Recognition. pp. 11444–11453 (2023)